The NuSTAR view of Radio-Quiet AGN

Andrea Marinucci
(Università degli Studi Roma Tre)
on behalf of the
NuSTAR AGN Physics WG

The 40th COSPAR Scientific Assembly
Moscow, 2-10 August 2014

Outline

- Brief introduction about scientific goals
- Radio-quiet AGN seen by NuSTAR
- Results
- Conclusions

Outline

- Brief introduction about scientific goals
- Radio-quiet AGN seen by NuSTAR
- Results
- Conclusions

Introduction – Primary emission

One of the main open problem for AGN is the nature of the primary X-ray emission.

It is due to Comptonization of soft photons, but the geometry, optical depth and temperature of the emitting corona are largely unknown.

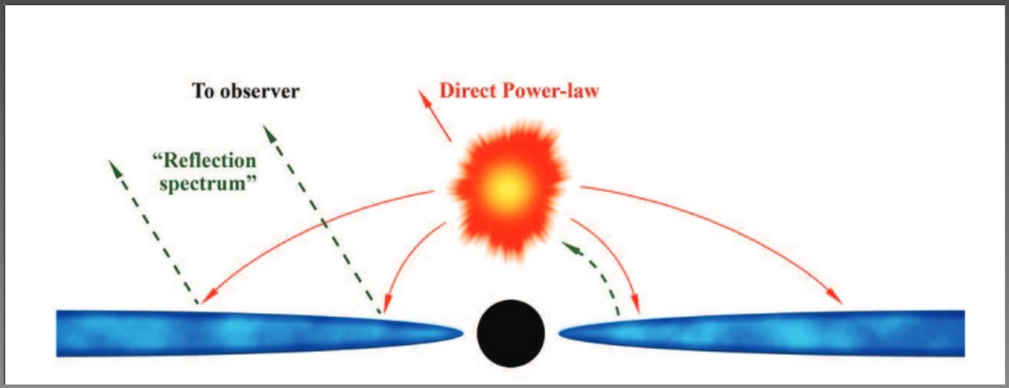

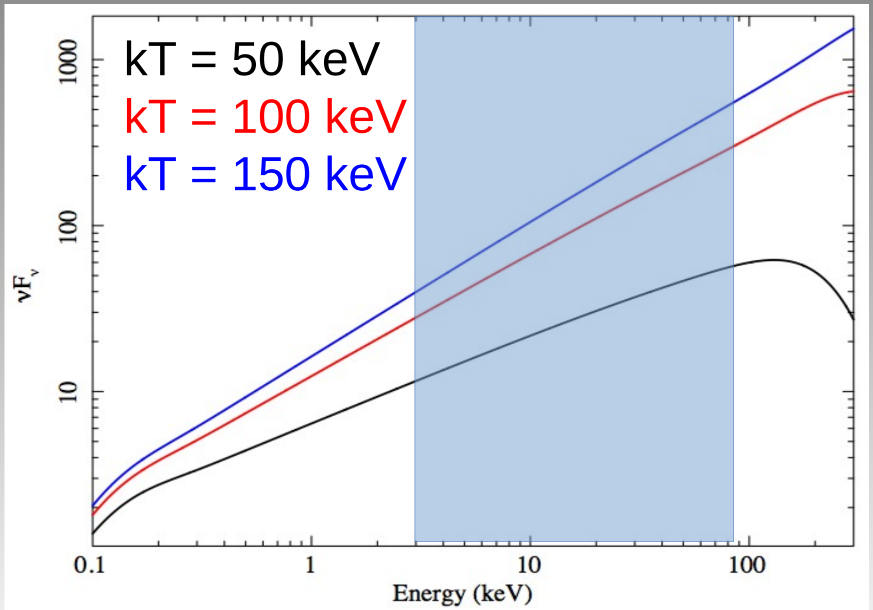

Most popular models imply E_{cut}=2-3 kT, so measuring E_{cut} helps constraining Comptonization models.

Introduction – Primary emission

So far, we have only a handful of results based on non focusing, and therefore strongly background-dominated, satellites (BeppoSAX-PDS, Suzaku HXD-PIN, INTEGRAL, Swift-BAT)

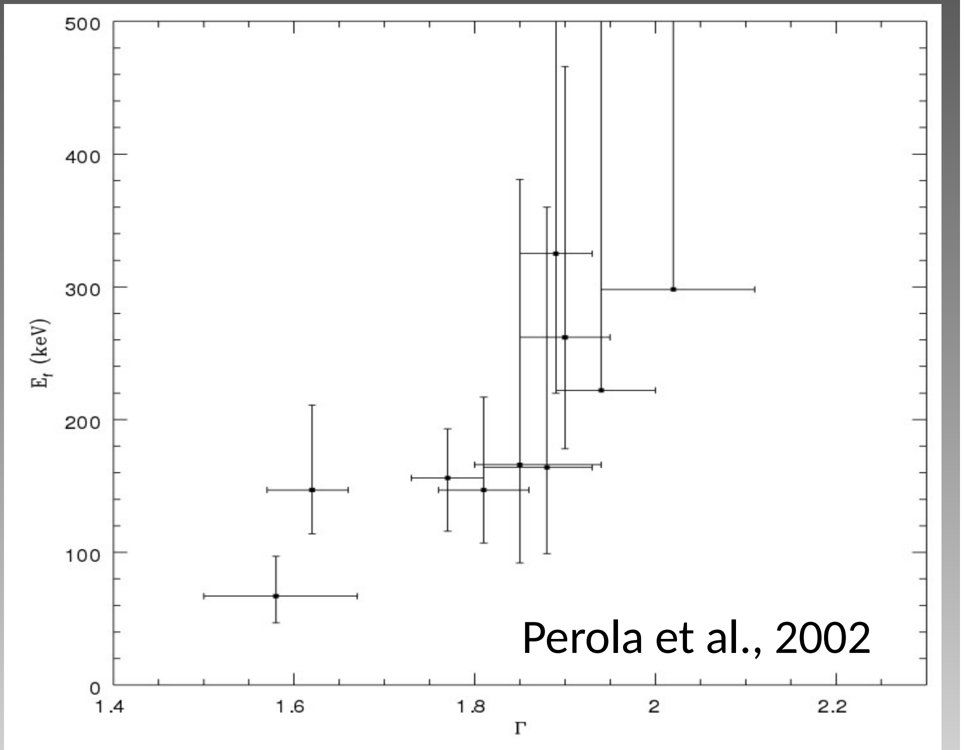

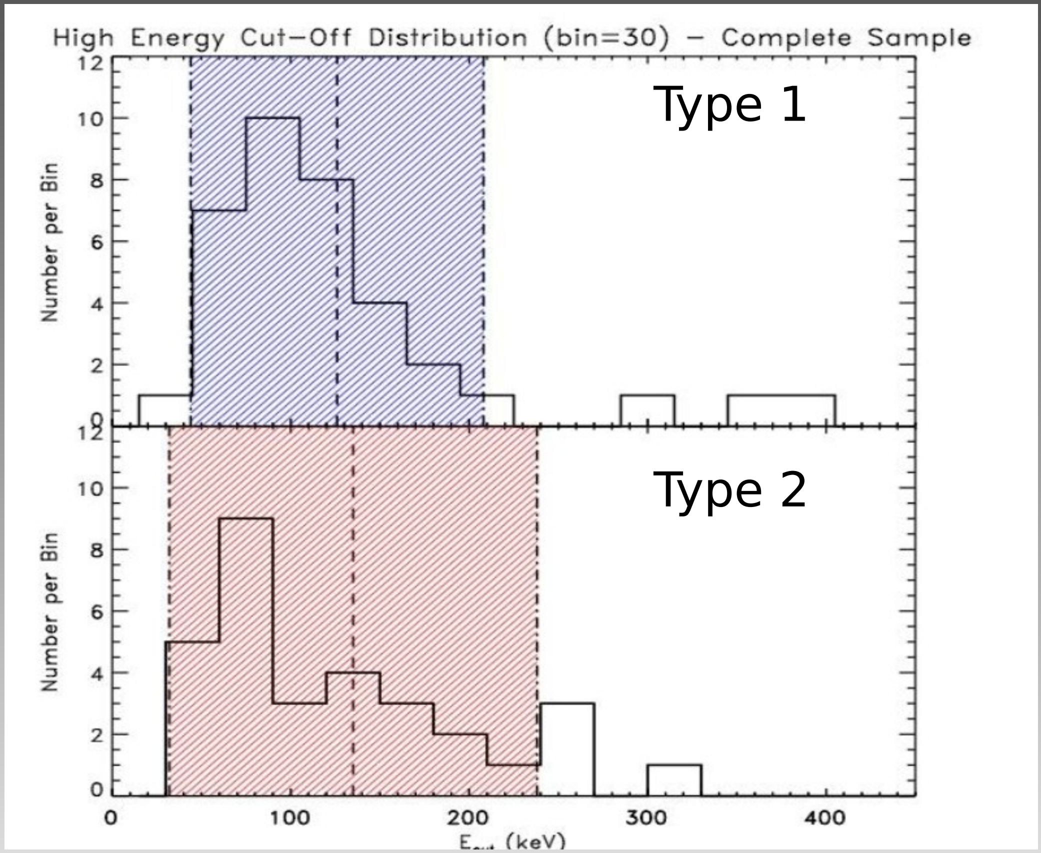

De Rosa et al. 2012, Molina et al. 2013

Introduction – Relativistic reflection

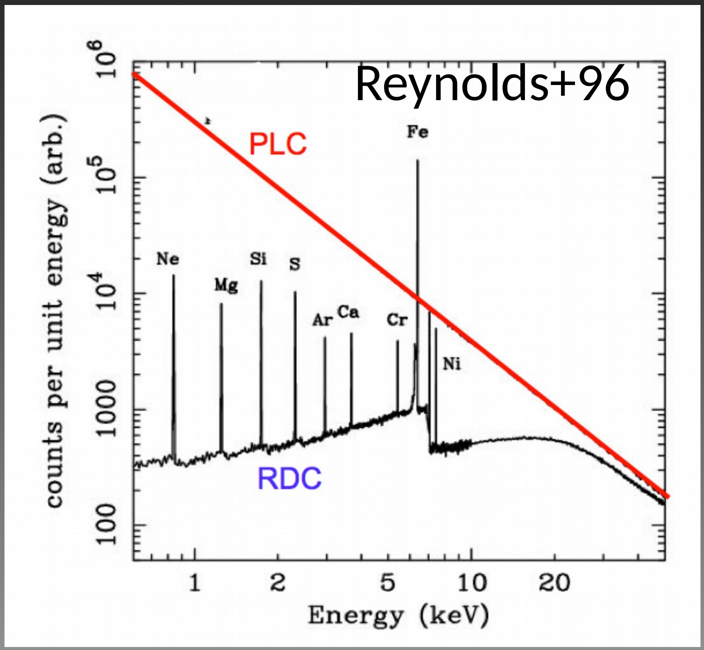

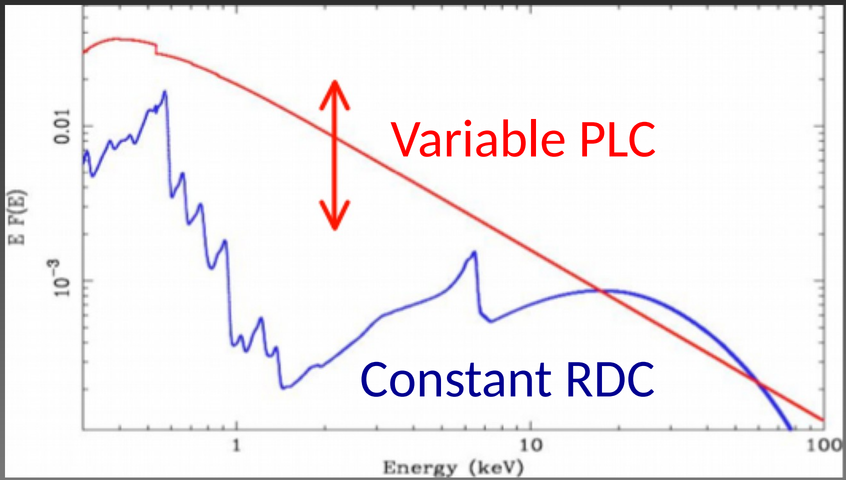

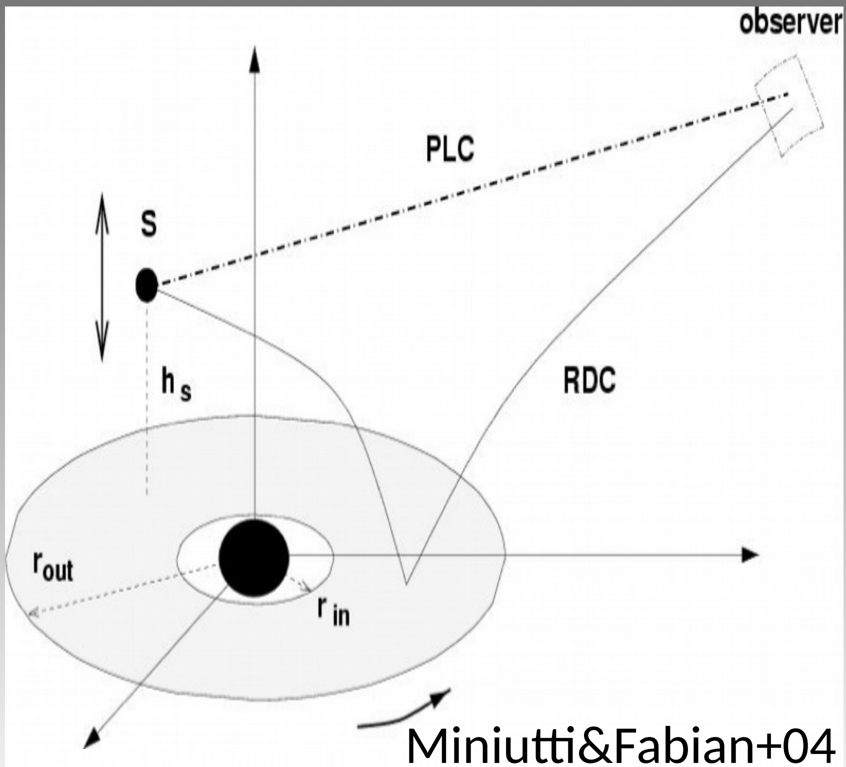

Light bending model:
much of the flux is bent onto the disk
giving a constant, strong RDC

Introduction – Relativistic reflection

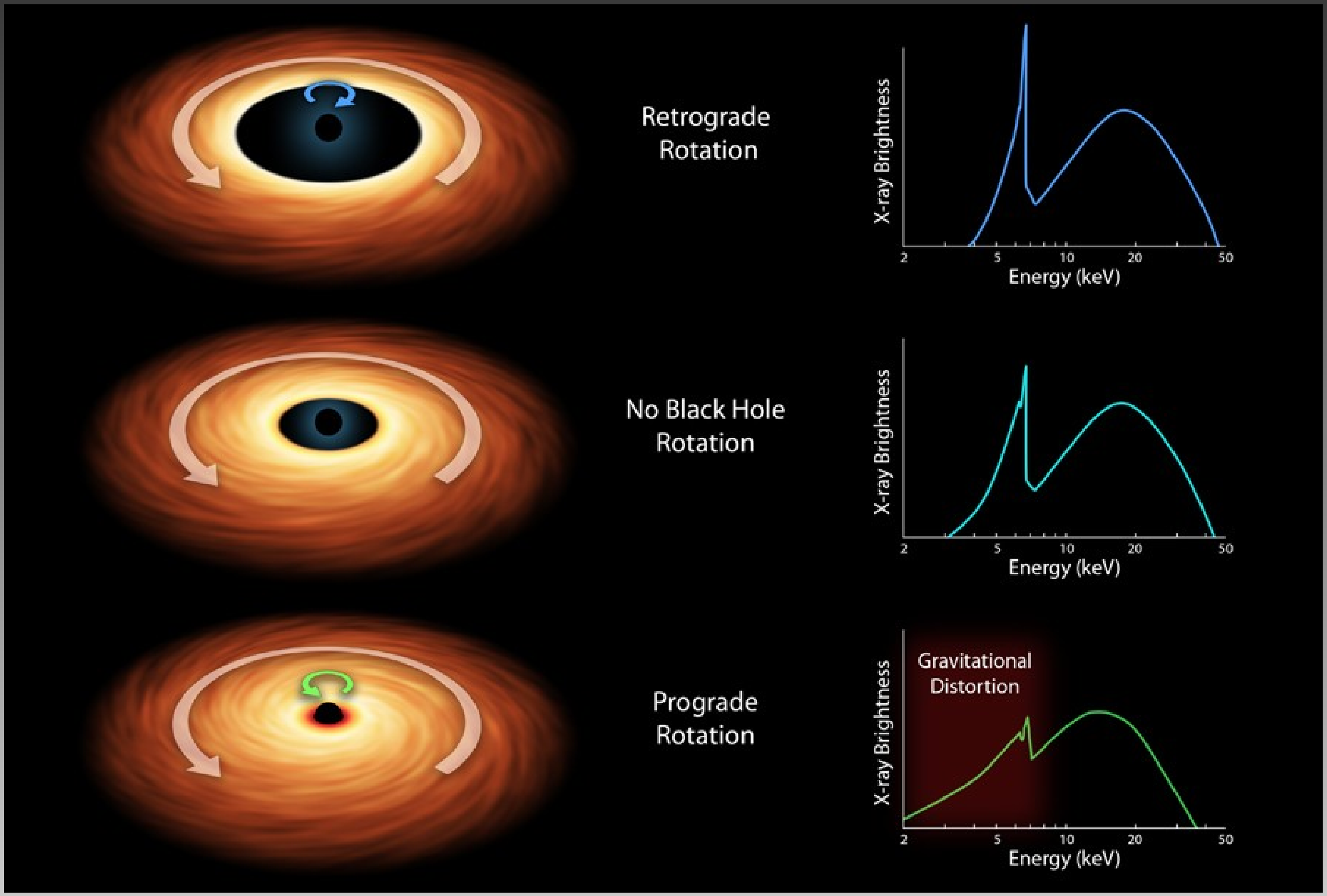

Spin alters shape of Fe Kα line and Compton hump in predictable, measurable ways.

Outline

- Brief introduction about scientific goals
- Radio-quiet AGN seen by NuSTAR
- Results
- Conclusions

The NuSTAR satellite

Nuclear Spectroscopic Telescope Array

1 Ms Sensitivity

- 3.2×10^{-15} erg/cm^2/s (6 – 10 keV)
- 1.4×10^{-14} erg/cm^2/s (10 – 30 keV)

Imaging

- HPD 58”
- FWHM 18”
- Localization 2” (1-sigma)

Spectral response

- energy range: 3-79 keV
- ΔE @ 6 keV 0.4 keV FWHM
- ΔE @ 60 keV 1.0 keV FWHM

Target of Opportunity

- response <24 hr
- typical 6-8 hours
- 80% sky accessibility

Harrison et al., 2013

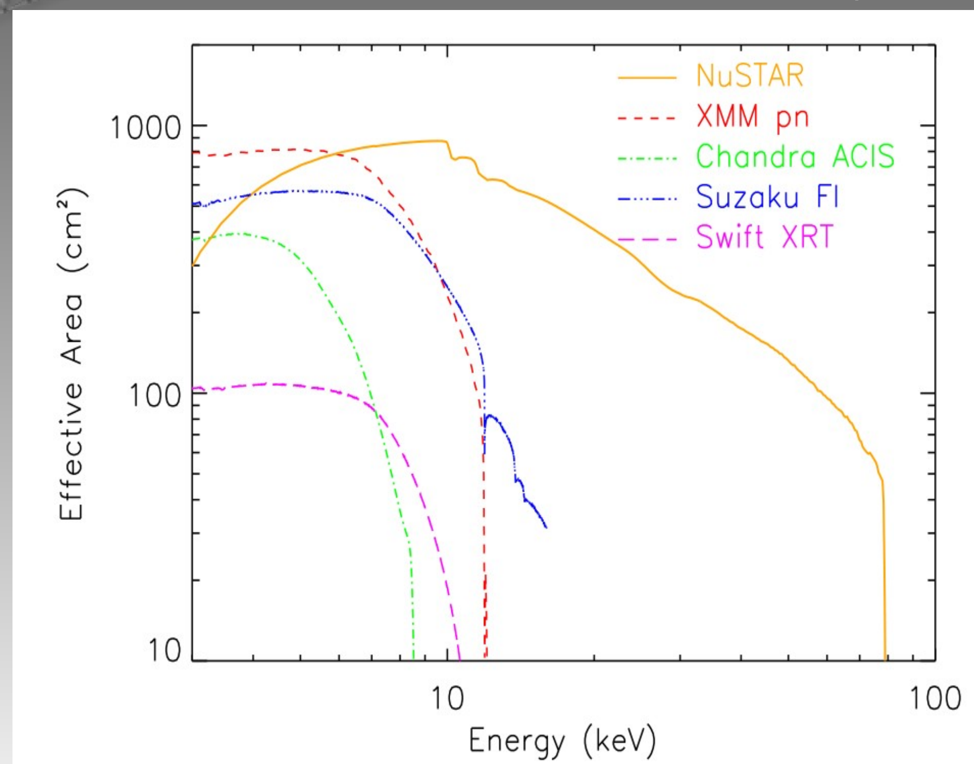

The NuSTAR satellite

The combination of NuSTAR high effective area and low background yelds ~100x better S/N versus Suzaku HXD-PIN

MCG-6-30-15: 125 ks net exposure time and same 15-70 keV flux (6.5×10^{-11} $erg/cm^2/s$)

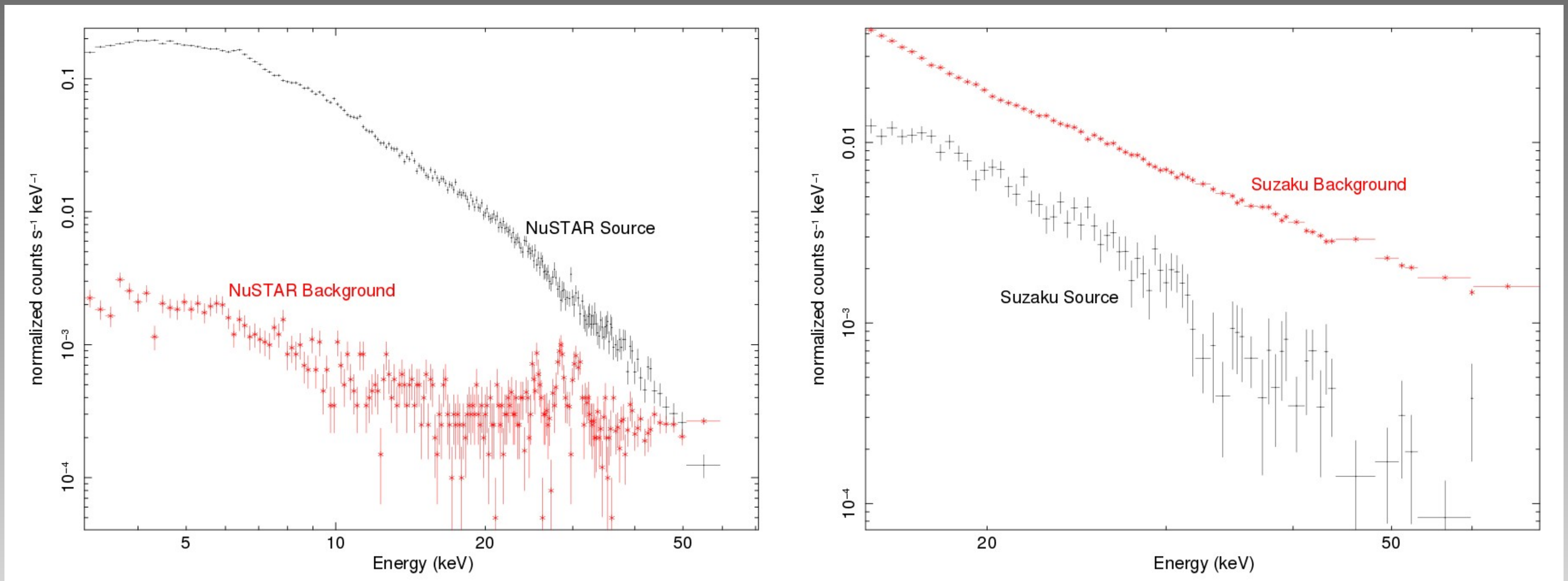

Marinucci et al., 2014a

Radio-quiet AGN observed by NuSTAR

Target	Exposure Time	Simultaneous	Reference
Ark 120	130 ks	XMM-Newton	Matt et al., 2014
IC 4329A	180 ks	Suzaku	Brenneman et al., 2014a,b
MCG—6-30-15	3x130ks	XMM-Newton	Marinucci et al., 2014a
Mrk 335	300 ks	Swift	Parker et al., 2014
NGC 1365	4x130 ks	XMM-Newton	Risaliti et al., 2013 Walton et al., 2014
SWIFT J2127.4	3x130ks	XMM-Newton	Marinucci et al., 2014b

Outline

- Brief introduction about scientific goals
- Radio-quiet AGN seen by NuSTAR
- Results
- Conclusions

The soft excess in Ark 120

Most AGN show soft X-ray emission in excess of the extrapolation of the hard primary emission

In many sources the soft excess is well explained by ionized reflection from the accretion disk (e.g. Walton et al. 2013)

However, there are sources in which another component is required (Patrick et al. 2012, Lohfink et al. 2012, Petrucci et al. 2013)

Ark 120 is one of them (Matt et al. 2014)

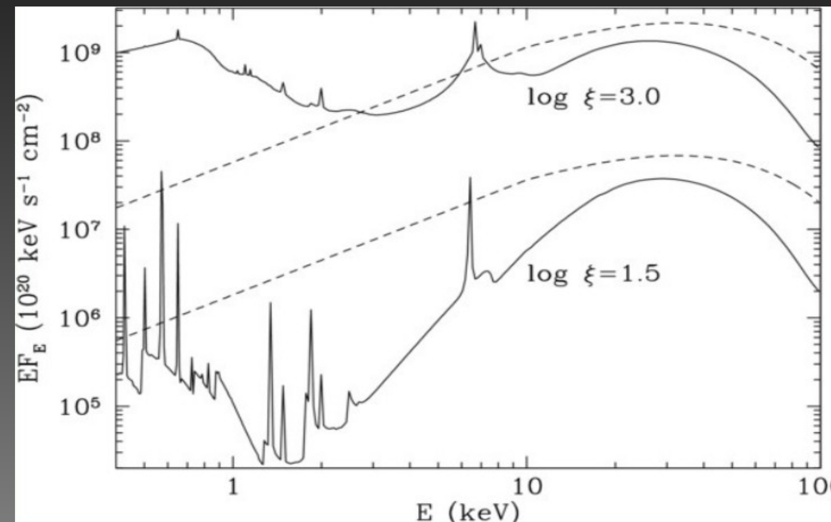

Ross & Fabian 2005

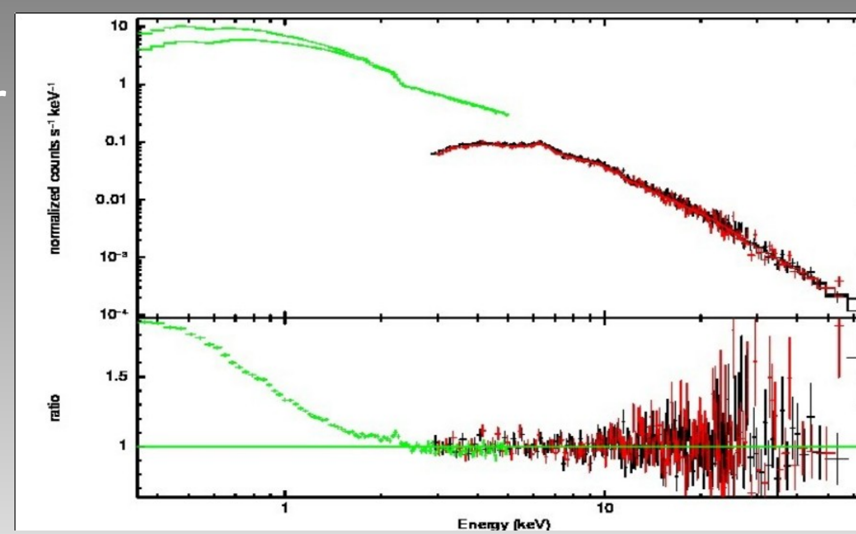

Matt et al. 2014

The soft excess in Ark 120

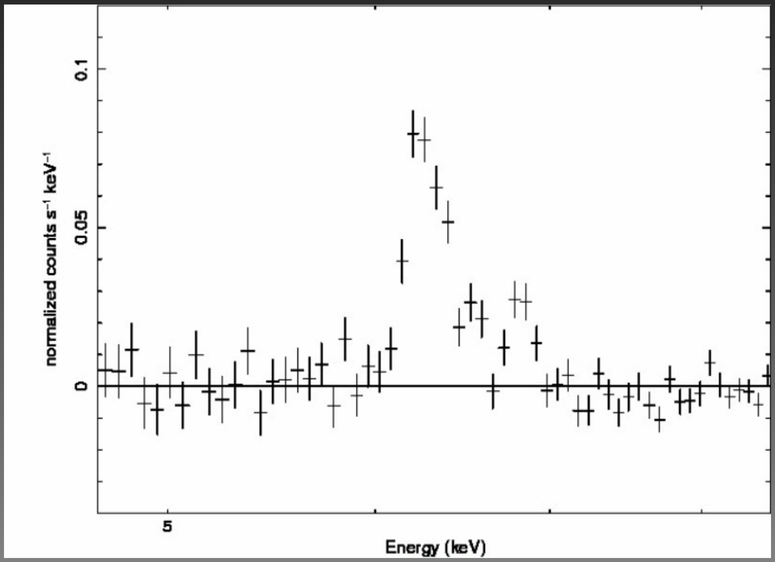

Matt et al. 2014

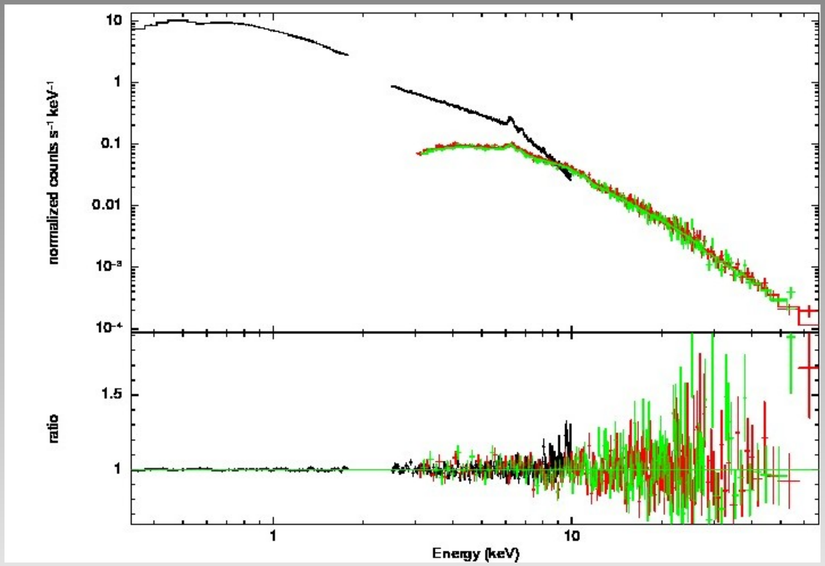

No obvious evidence for a relativistic Iron line (differently from a previous Suzaku observation, Nardini et al. 2011)

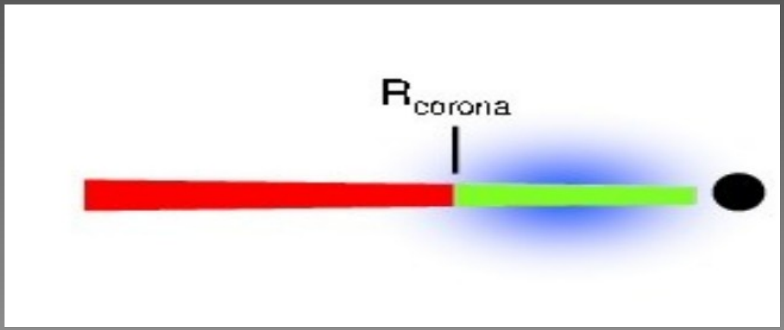

The broad-band best fit is with a Comptonization model for the soft excess. Optxagnf
(Done et al. 2012) is a disk/corona emission model which assumes a thermal disk emission outside the coronal radius, and soft and hard Comptonization inside.

The soft excess in Ark 120

Fluxes from the Optical Monitor on board on XMM-Newton support an intermediate value for the black hole spin.

Matt et al. 2014

a	0	0.50	0.99
L/L_{Edd}	$0.16^{+0.16}_{-0.08}$	$0.05^{+0.01}_{-0.01}$	$0.04^{+0.03}_{-0.01}$
R_c (R_G)	$11.5^{+0.1}_{-3.4}$	$31.3^{+39.2}_{-16.6}$	$24.9^{+16.0}_{-15.2}$
kT (keV)	$0.33^{+0.02}_{-0.02}$	$0.32^{+0.01}_{-0.01}$	$0.32^{+0.02}_{-0.01}$
τ	$12.9^{+1.1}_{-0.9}$	$13.6^{+0.6}_{-0.2}$	$13.6^{+0.4}_{-0.7}$
Γ	$1.73^{+0.02}_{-0.02}$	$1.73^{+0.02}_{-0.02}$	$1.73^{+0.02}_{-0.02}$
E_c (keV)	>190	>190	>190

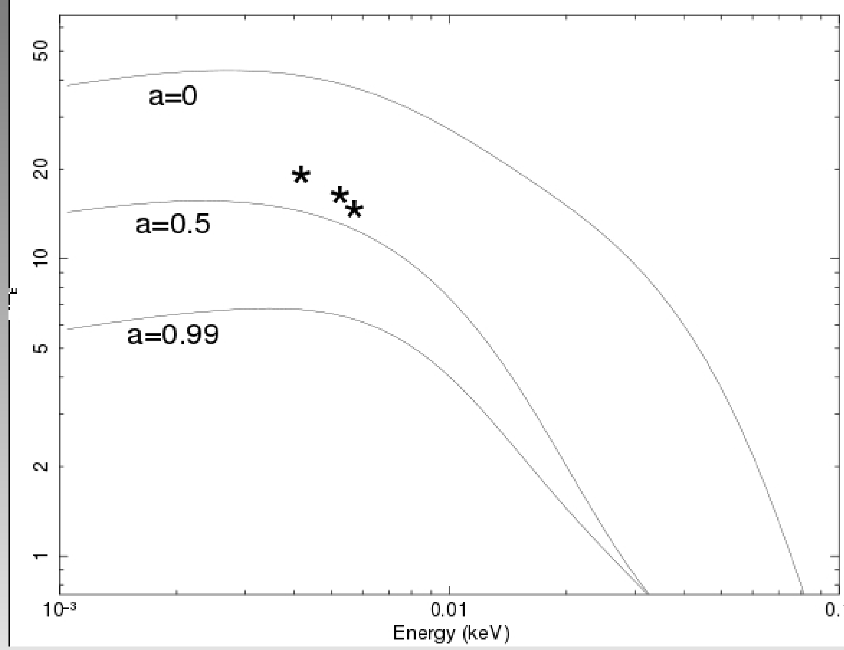

Coronal parameters in IC 4329A

-Bright Sy1 galaxy, $F_{2\text{-}10\ keV}$ ~ 0.1-1.8 x10^{-10} erg/cm^2/s

- E_c=100^{+200}_{-40} keV (INTEGRAL+XMM, Molina+13)

- Observed simultaneously by NuSTAR and Suzaku for ~120 ks in 2012

Brenneman et al. 2014b

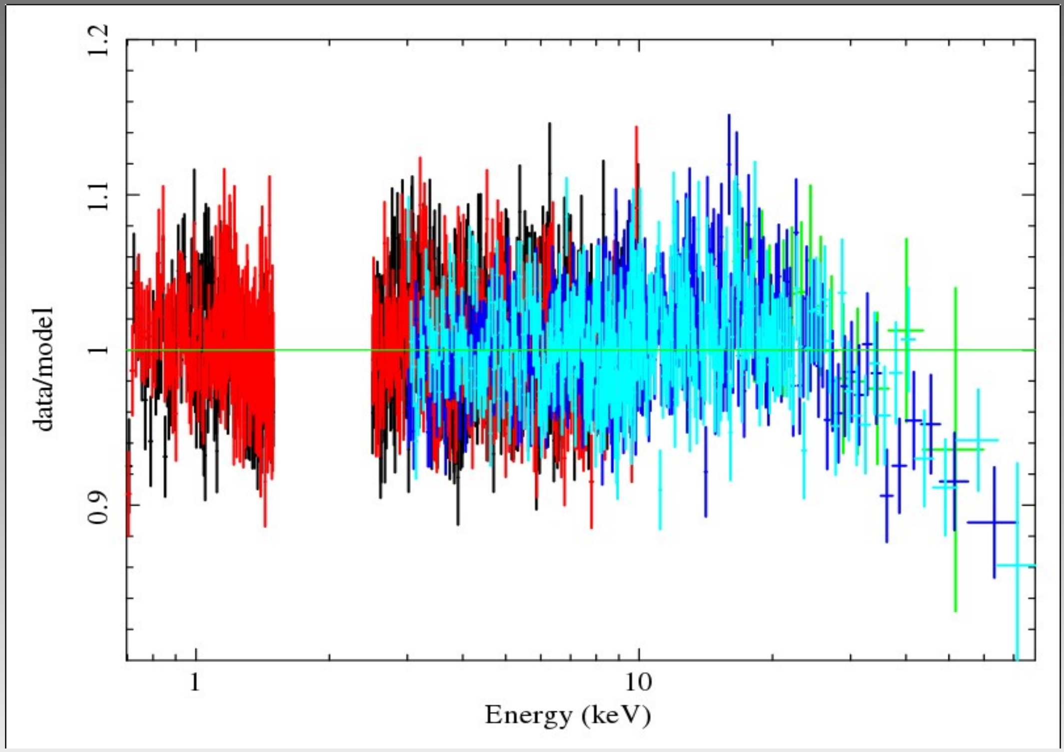

When a model composed of a primary continuum+reflection is applied to the data some residuals at high energies are found.

Coronal parameters in IC 4329A

Component	Parameter (units)		SPHERE	SLAB
TBabs	$N_H\,(cm^{-2})$	$4.61 \times 10^{20}(f)$	$4.61 \times 10^{20}(f)$	$4.61 \times 10^{20}(f)$
XSTAR grid	$N_H\,(cm^{-2})$	$6.03 \pm 0.13 \times 10^{21}$	$6.02 \pm 0.13 \times 10^{21}$	$6.00^{+0.12}_{-0.13} \times 10^{21}$
	$\log\xi\,(erg\,cm\,s^{-1})$	0.73 ± 0.02	0.73 ± 0.02	0.73 ± 0.02
zpo	Γ	1.73 ± 0.01	$1.73(f)$	$1.73(f)$
	$E_{cut}\,(keV)$	186^{+14}_{-14}	---	---
	$K_{po}\,(ph\,cm^{-2}\,s^{-1})$	$2.82 \pm 0.03 \times 10^{-2}$	---	---
compTT	$kT_e\,(keV)$	---	50^{+6}_{-3}	61 ± 1
	τ	---	$2.34^{+0.16}_{-0.21}$	0.68 ± 0.02
	$K_{comptt}\,(ph\,cm^{-2}\,s^{-1})$	---	$5.46^{+0.38}_{-0.54} \times 10^{-3}$	$4.46 \pm 0.11 \times 10^{-3}$
xillver	Fe/solar	$1.51^{+0.29}_{-0.28}$	$1.51^{+0.28}_{-0.27}$	$1.50^{+0.28}_{-0.27}$
	Γ	$1.73*$	$1.73(f)$	$1.73(f)$
	$K_{refl}\,(ph\,cm^{-2}\,s^{-1})$	$2.79 \pm 0.20 \times 10^{-4}$	$2.74 \pm 0.18 \times 10^{-4}$	$2.89 \pm 0.18 \times 10^{-4}$

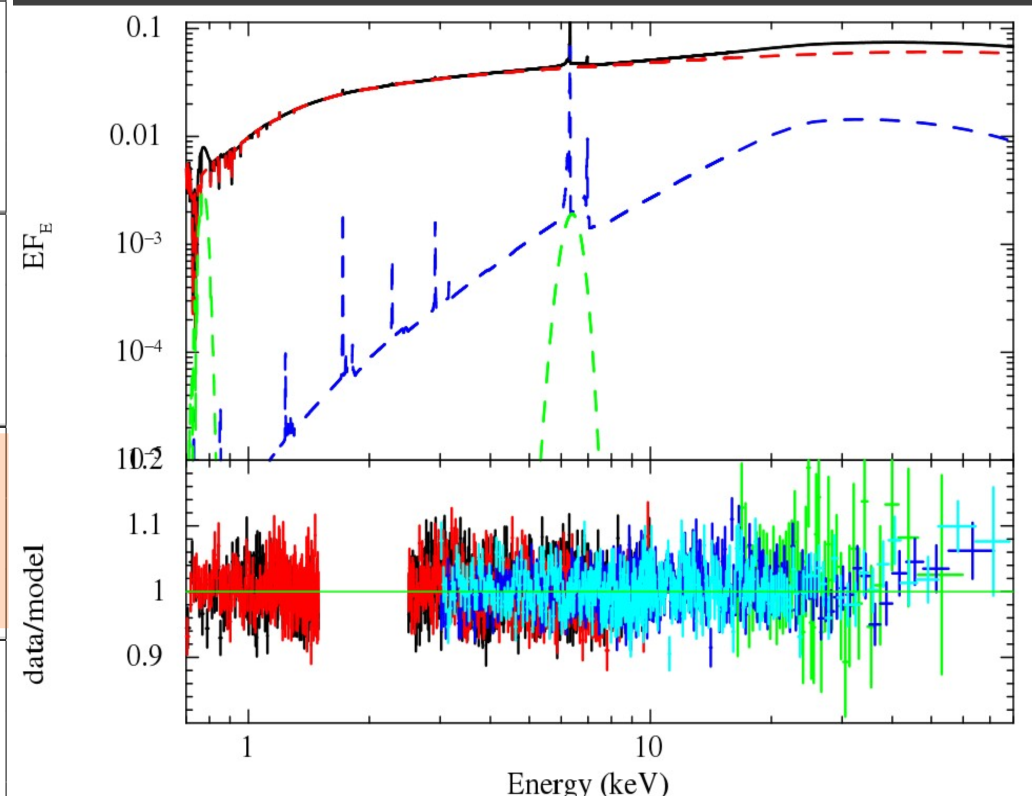

No evidence for relativistic lines.
Iron line and Compton reflection both originate from distant material.

Relativistic reflection in MCG—6-30-15

First broad Fe Ka line ever observed (Tanaka+95) and interpreted as originating from a rapidly spinning BH (Iwasawa+96)

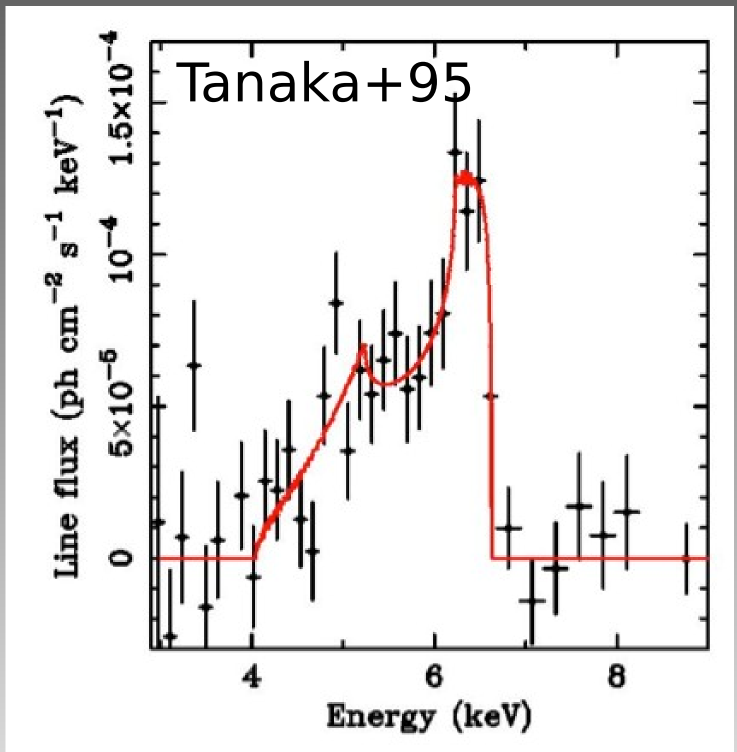

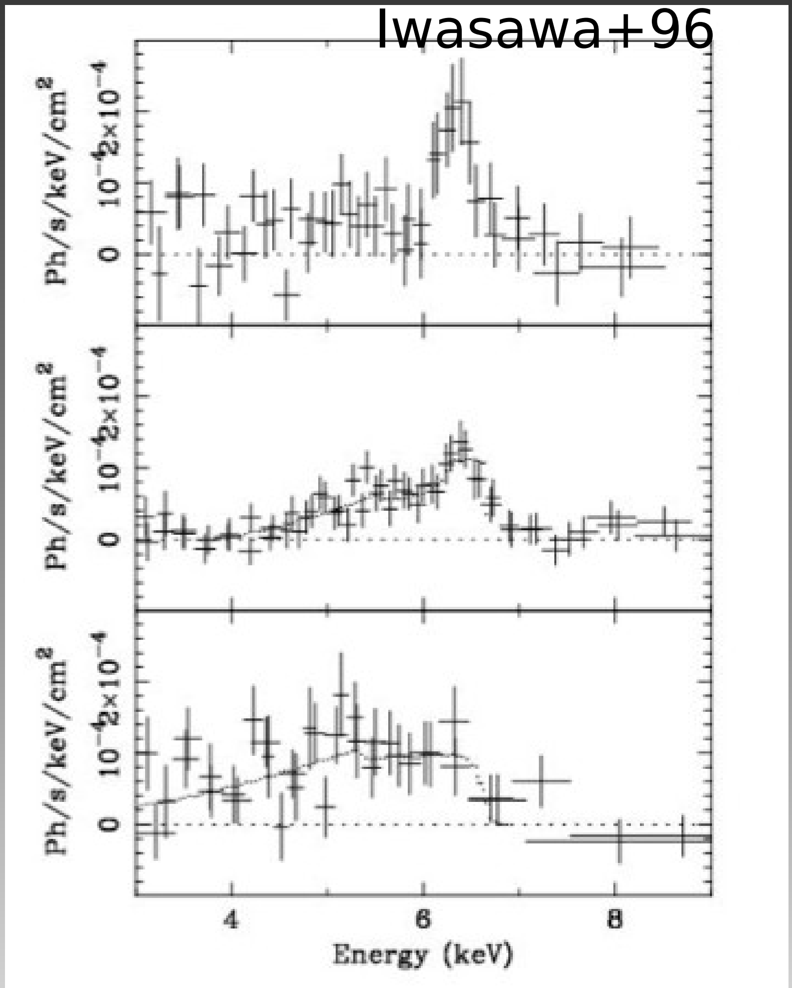

Relativistic reflection in MCG—6-30-15

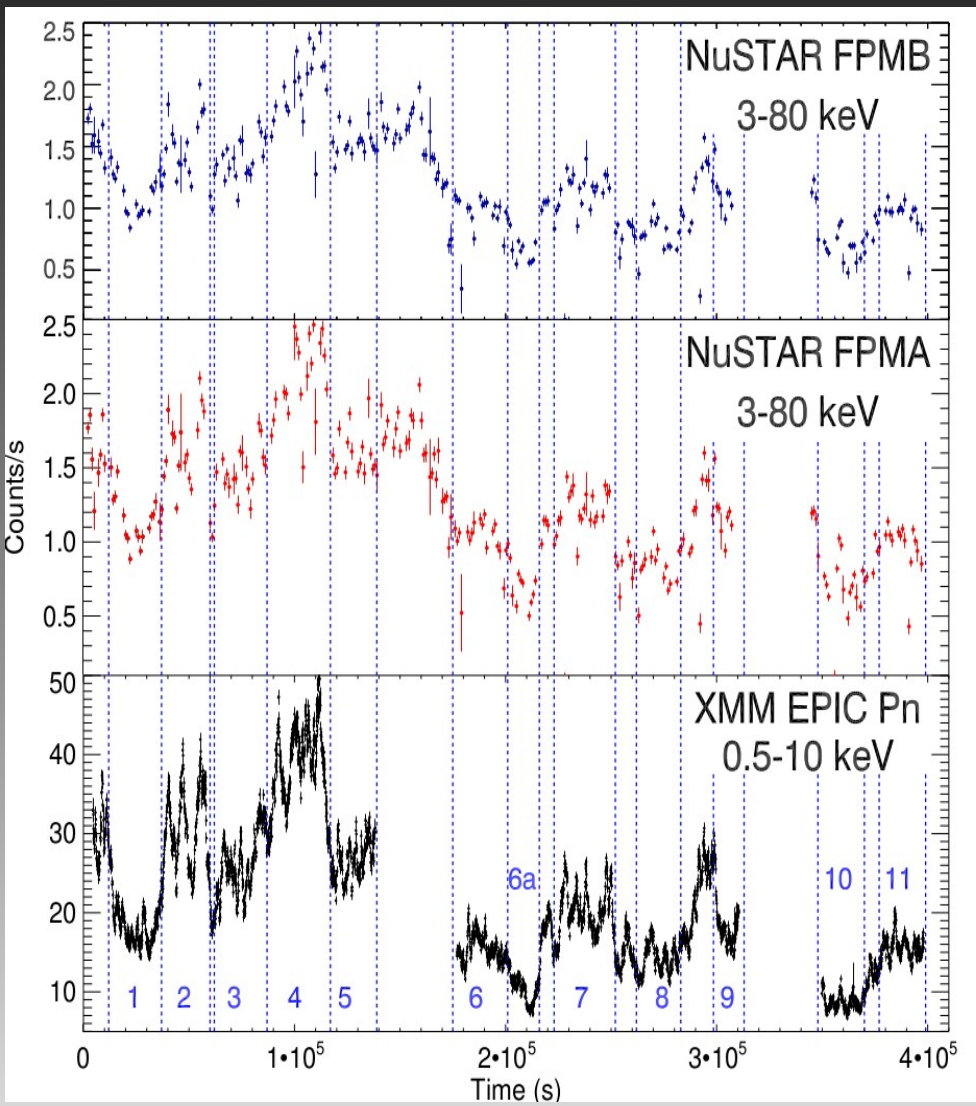

Marinucci et al. 2014a

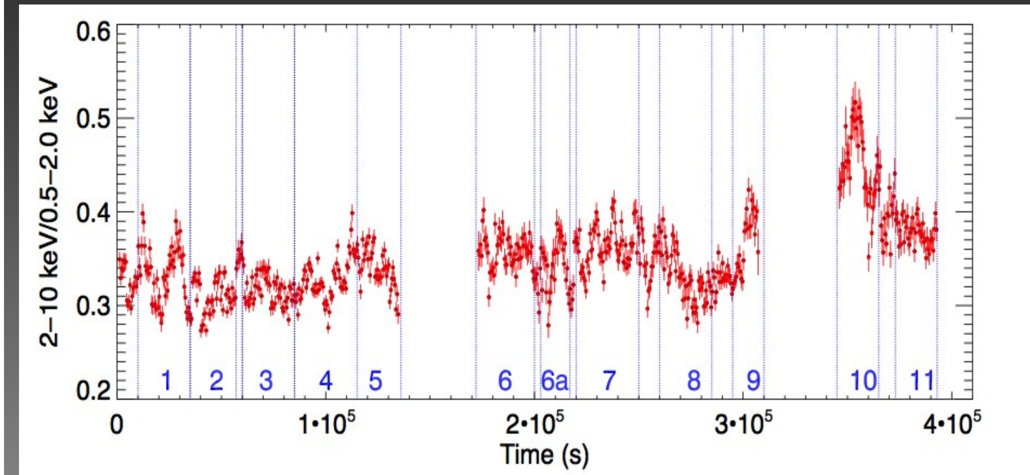

FIG. 3.— Ratio between the 2-10 keV and 0.5-2.0 keV light curves (in 500 s bins) and time intervals chosen for our analysis. Data are from *XMM-Newton* EPIC-Pn camera only and time is from the start of the observation.

The source has been observed in a very bright and variable state in 2013 during the XMM+NuSTAR campaign (Marinucci et al. 2014a)

Relativistic reflection in MCG—6-30-15

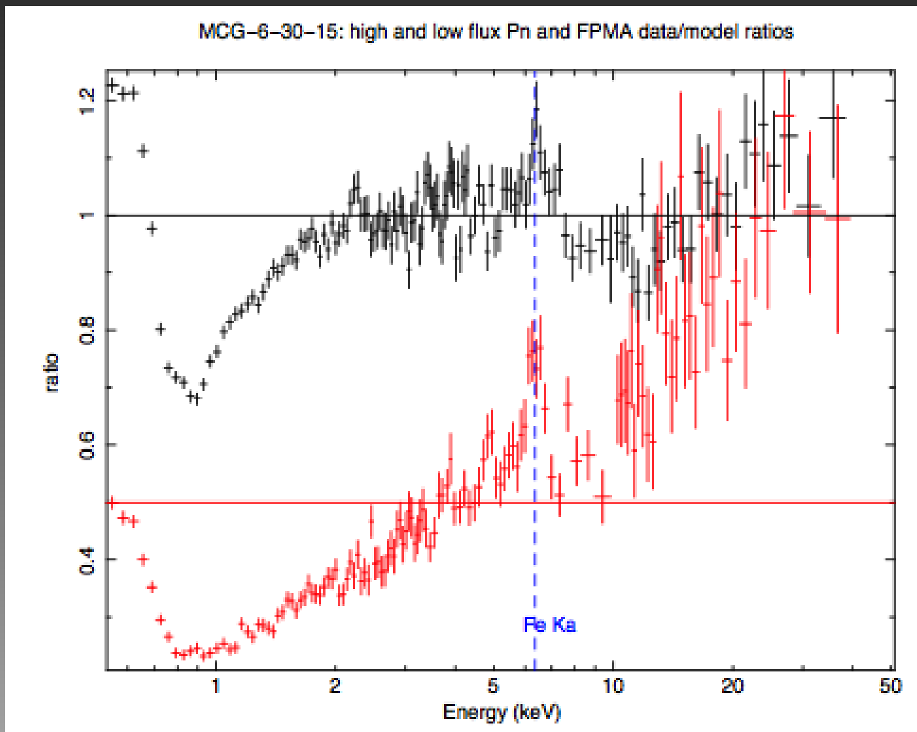

Marinucci et al. 2014a

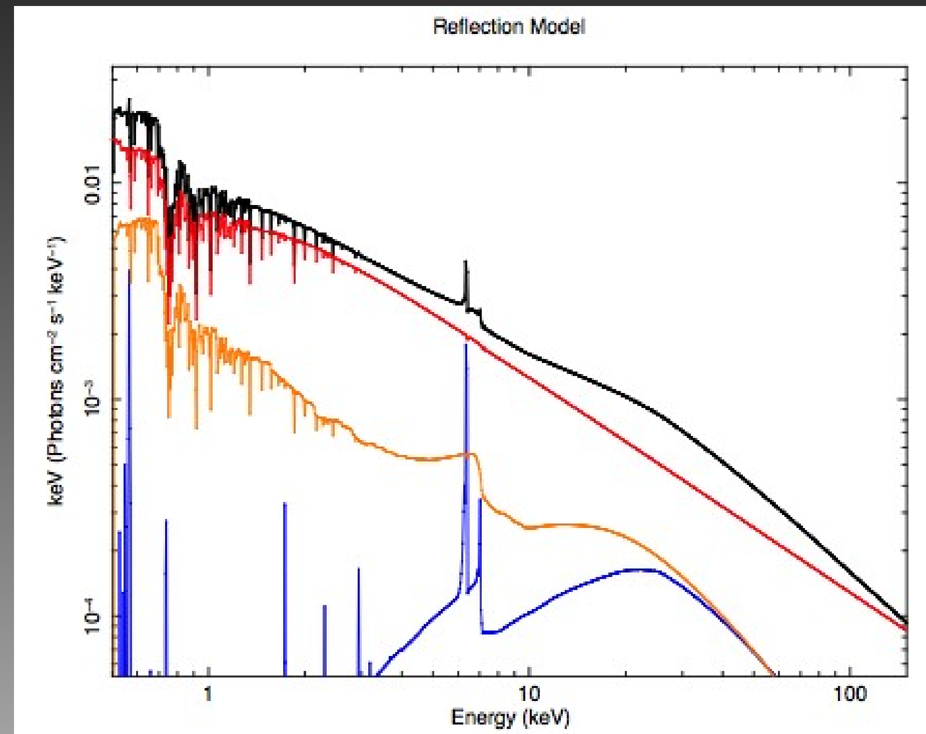

The different spectral shape in the time intervals considered is explained in terms of the interaction between the primary continuum and the accretion disk. A black hole spin of $a=0.91^{+0.06}_{-0.07}$ is measured.

Relativistic reflection in Mrk 335

Mrk 335 was observed by NuSTAR and Swift in a very faint state, allowing us to study the reflection properties of the source.

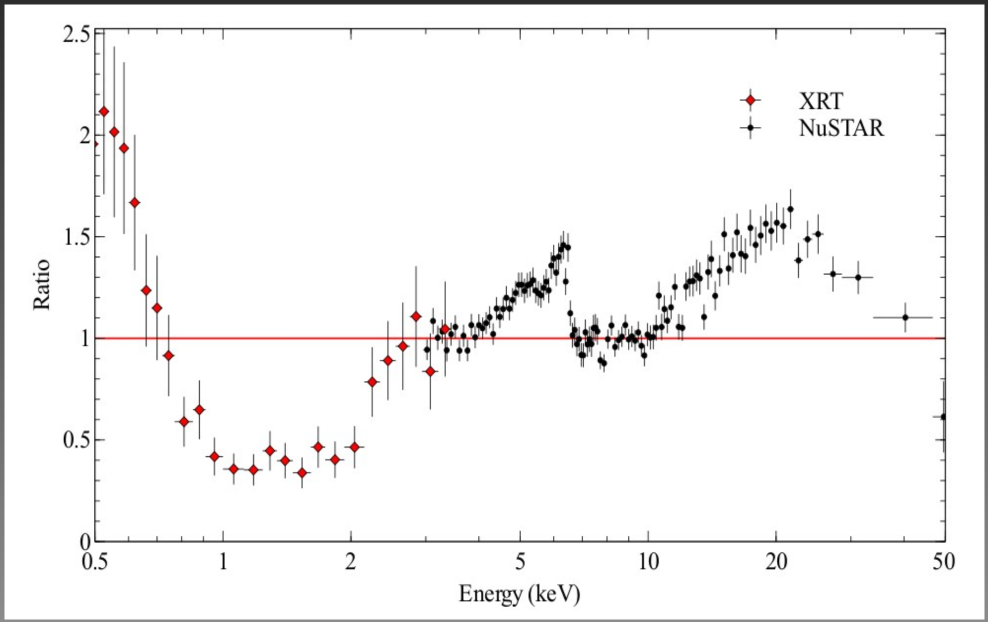

Parker et al. 2014

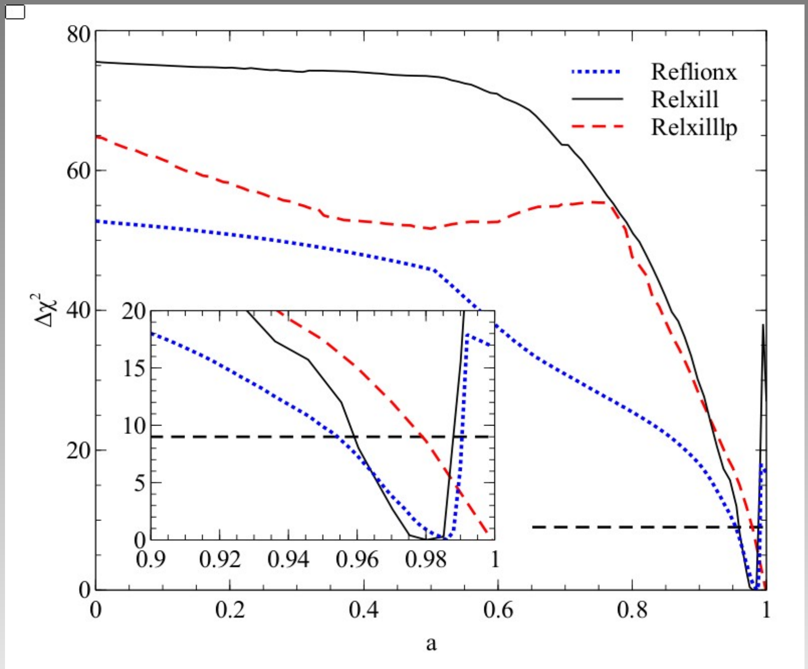

When flux-resolved states are considered a maximally rotating black hole spin is measured.

Black hole spin in NGC 1365

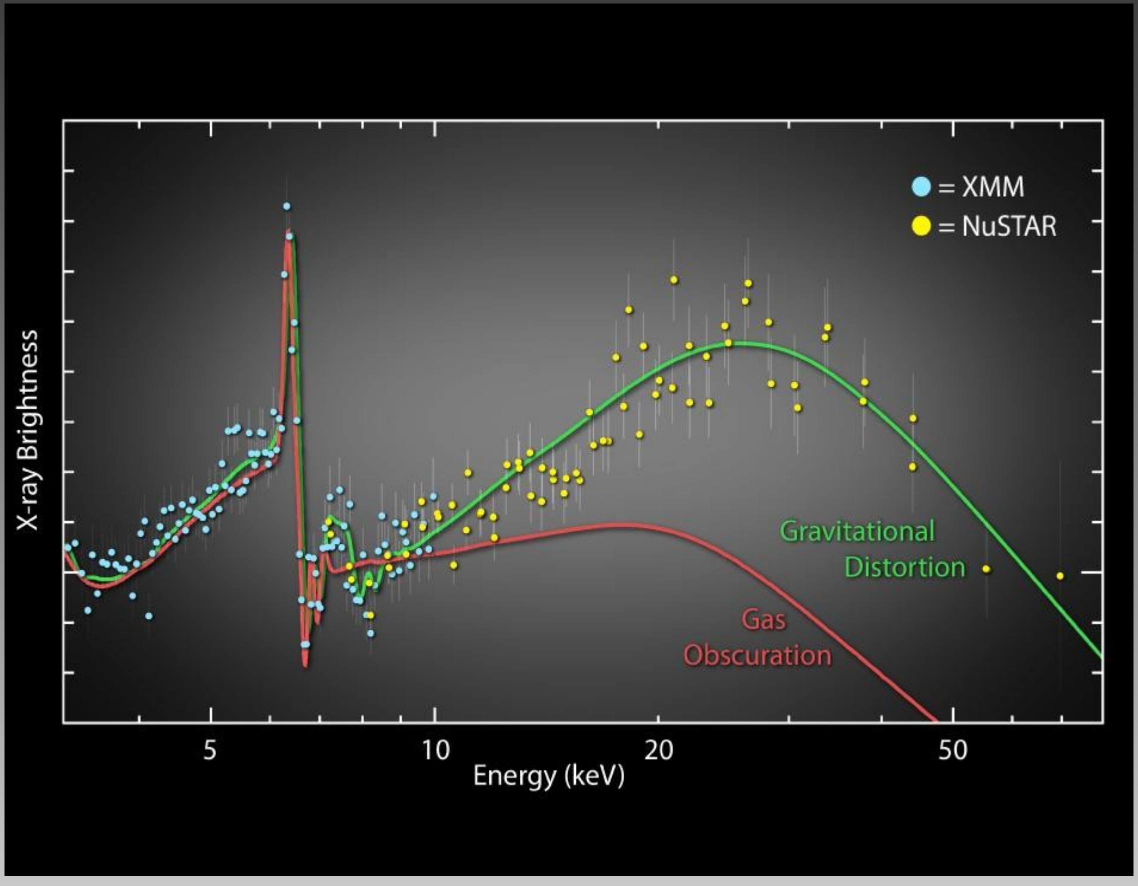

Risaliti et al. 2013, Nature

NGC 1365: a source in which both absorption and relativistic reflection play a major role in the X-rays

The first NuSTAR published paper is the spin measurement in NGC 1365

Black hole spin in NGC 1365

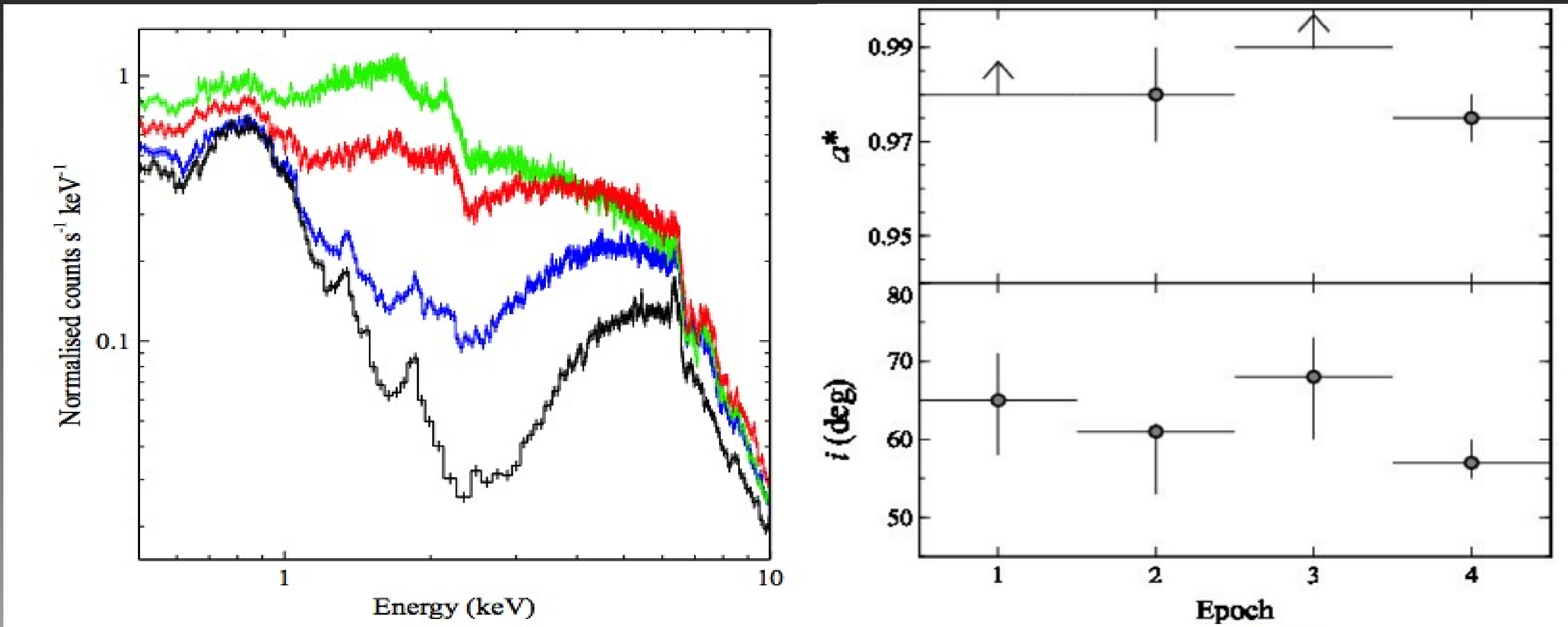

Walton et al. 2014

NGC 1365 was observed by XMM and NuSTAR four times. Despite large variations in the absorbers, no variations in the spin and inclination are found, demonstrating the robustness of the result.

TABLE 3
THE BLACK HOLE SPIN AND DISK INCLINATION CONSTRAINTS OBTAINED FOR EACH OF THE FOUR OBSERVATIONS OF NGC 1365.

Observation	a^*	i (deg)
1	> 0.98	65^{+6}_{-7}
2	0.98 ± 0.01	61^{+1}_{-8}
3	> 0.99	68^{+5}_{-8}
4	0.975 ± 0.005	57^{+3}_{-2}

Relativistic reflection in SWIFT J2127.4

NLS1 with a relativistically broadened Fe Kα emission line (a=0.6±0.2), a steep continuum (Γ=2-2.4), E_c=30-90 keV, L_{bol}/L_{Edd}~0.18 (Miniutti+09, Malizia+08, Panessa+11, Sanfrutos+13)

It was observed simultaneously with XMM-Newton for ~300 ks and both a strong Compton Hump and a broad Fe Kα line are present

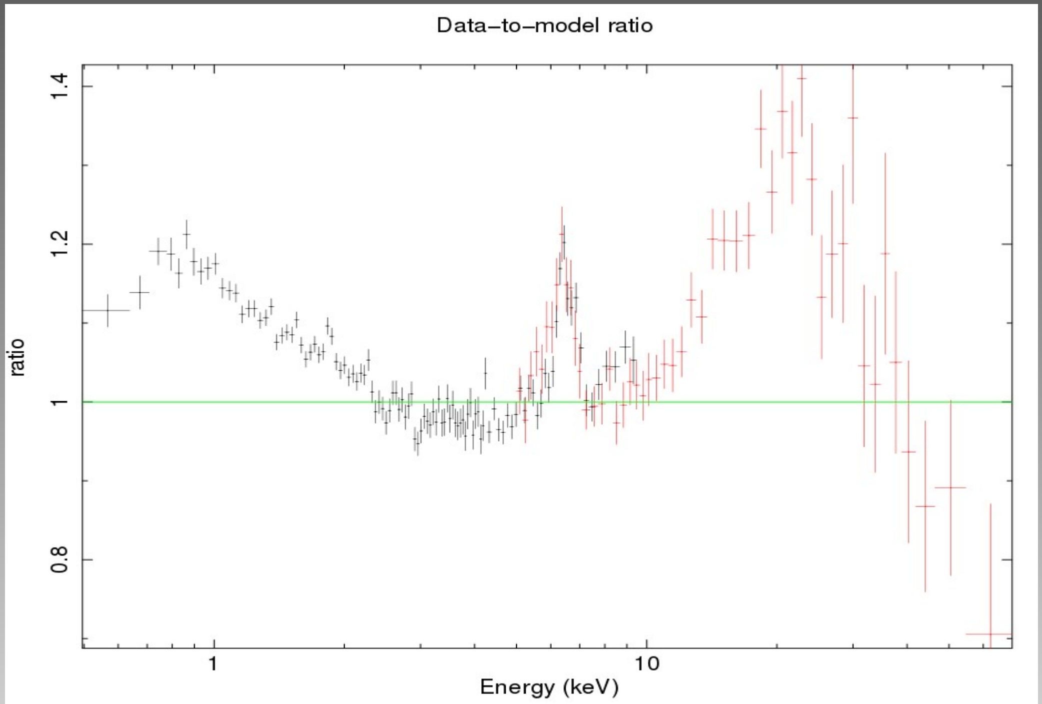

Marinucci et al. 2014b

Relativistic reflection in SWIFT J2127.4

When a model composed of a primary continuum, relativistic and distant reflection components is applied to the data the only residuals are above ~25 keV

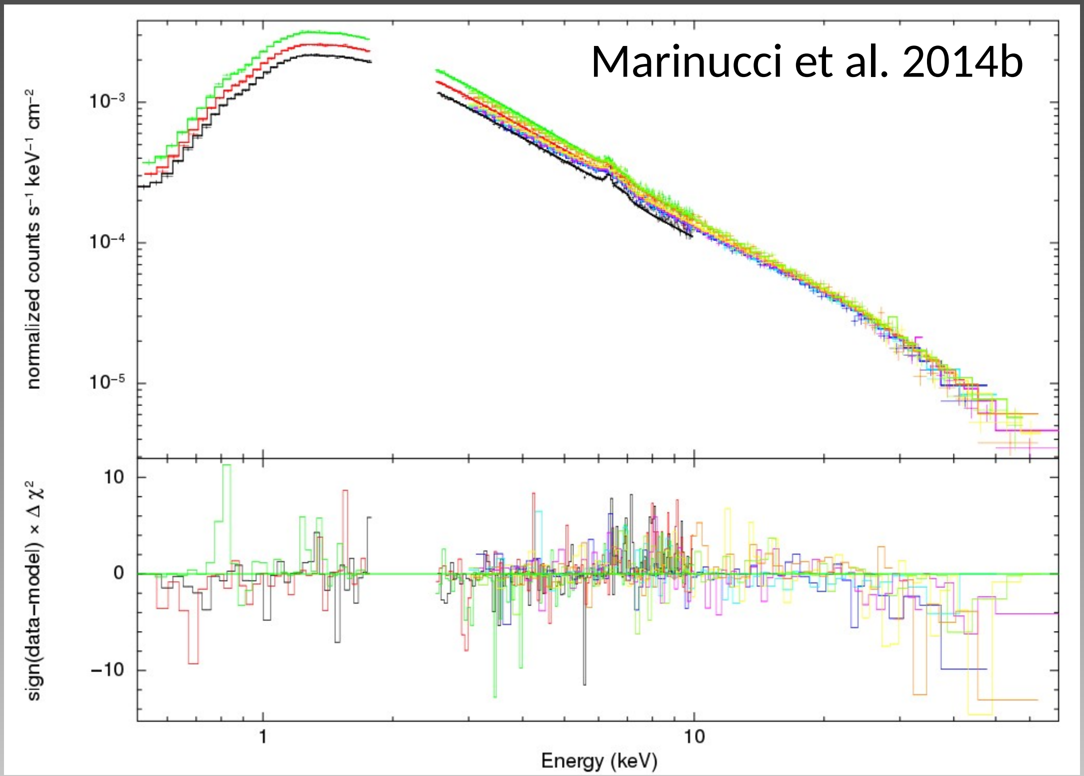

Relativistic reflection in SWIFT J2127.4

When a model composed of a primary continuum, relativistic and distant reflection components is applied to the data the only residuals are above ~25 keV

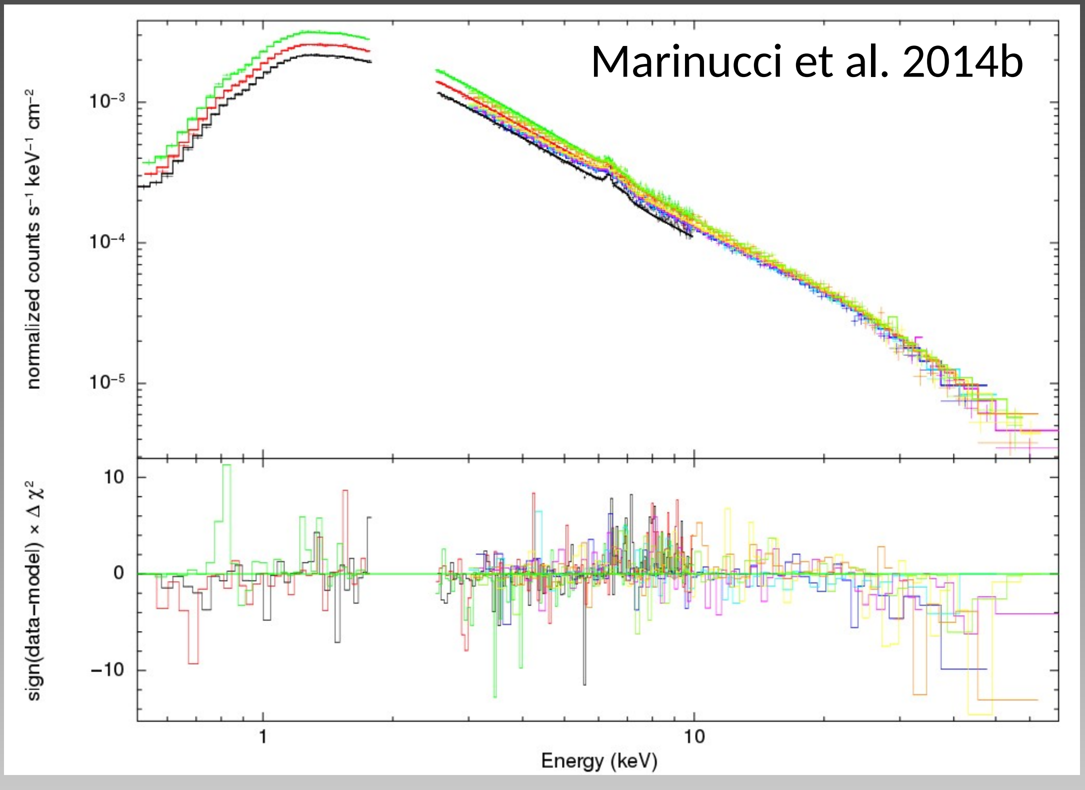

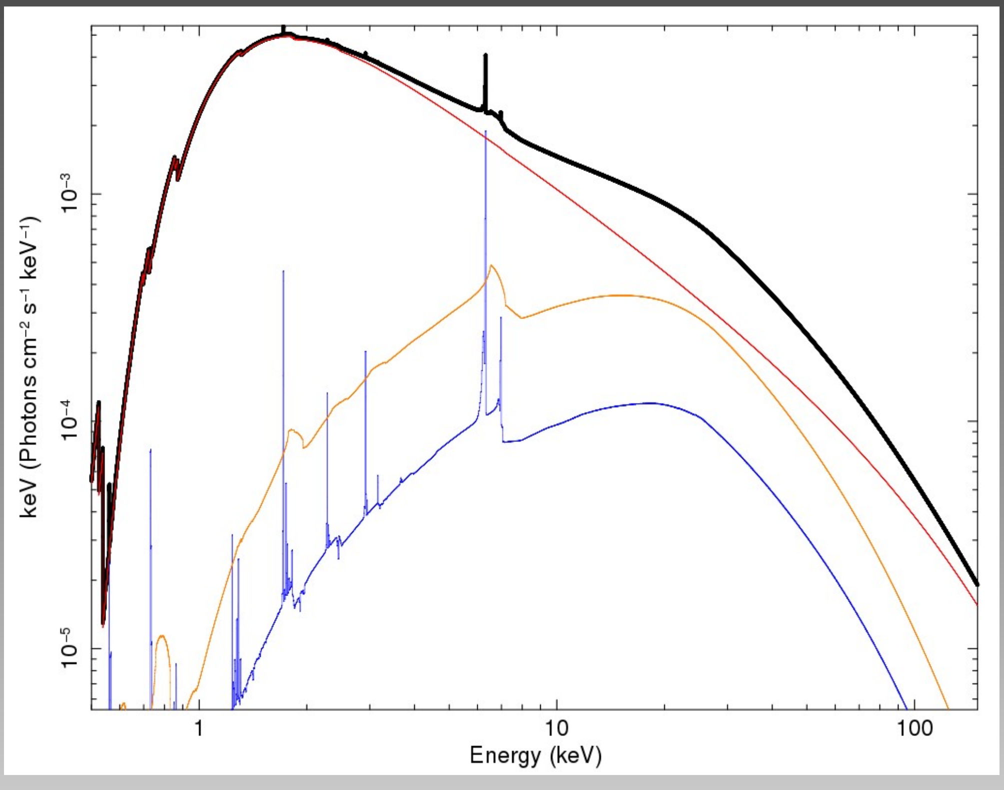

The inclusion of relxill model (Garcia & Dauser +14) allows us to measure a cutoff energy E_c=108±10 keV and to infer the contribution of the disk to the Compton hump.

Relativistic reflection in SWIFT J2127.4

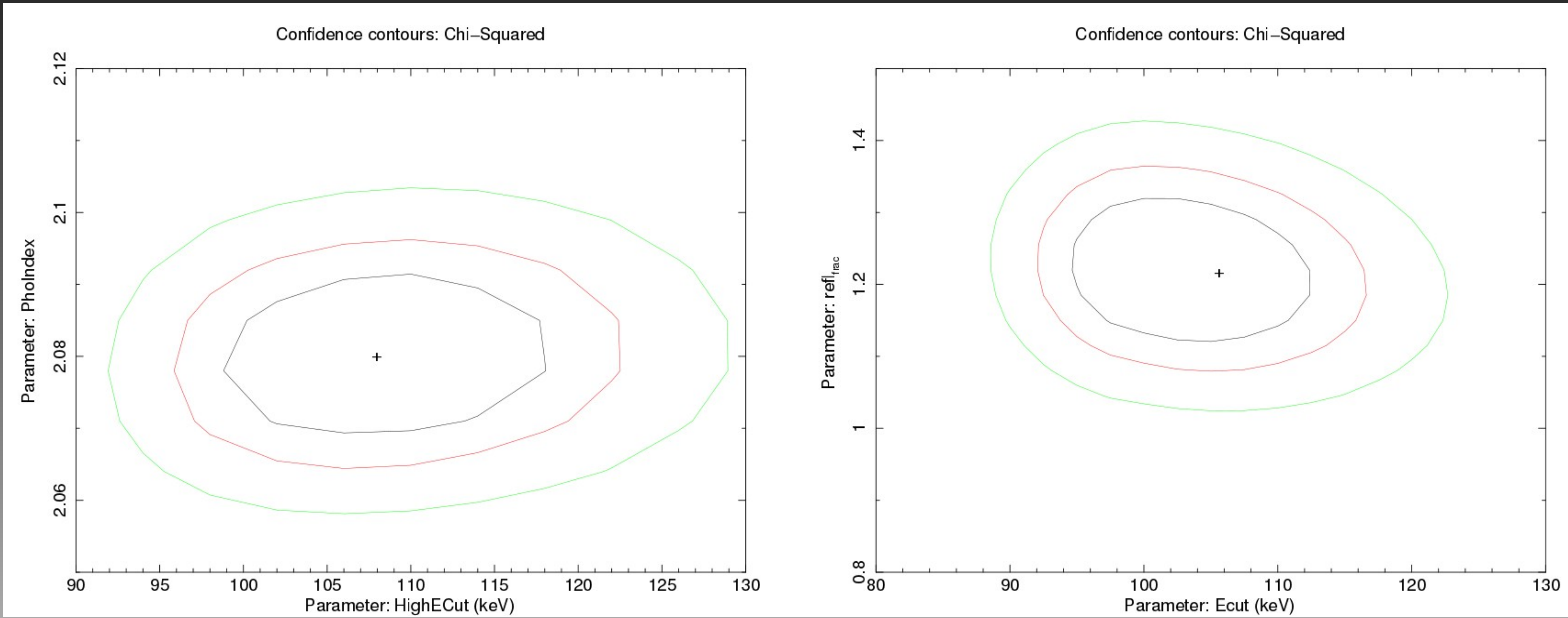

Using compTT (Titarchuk+94) with two different geometries we get:

SLAB	SPHERE
$kT_e=68^{+37}_{-32}$ keV	$kT_e=53^{+28}_{-26}$ keV
$\tau=0.35^{+0.35}_{-0.19}$	$\tau=1.35^{+1.03}_{-0.67}$

Relativistic reflection in SWIFT J2127.4

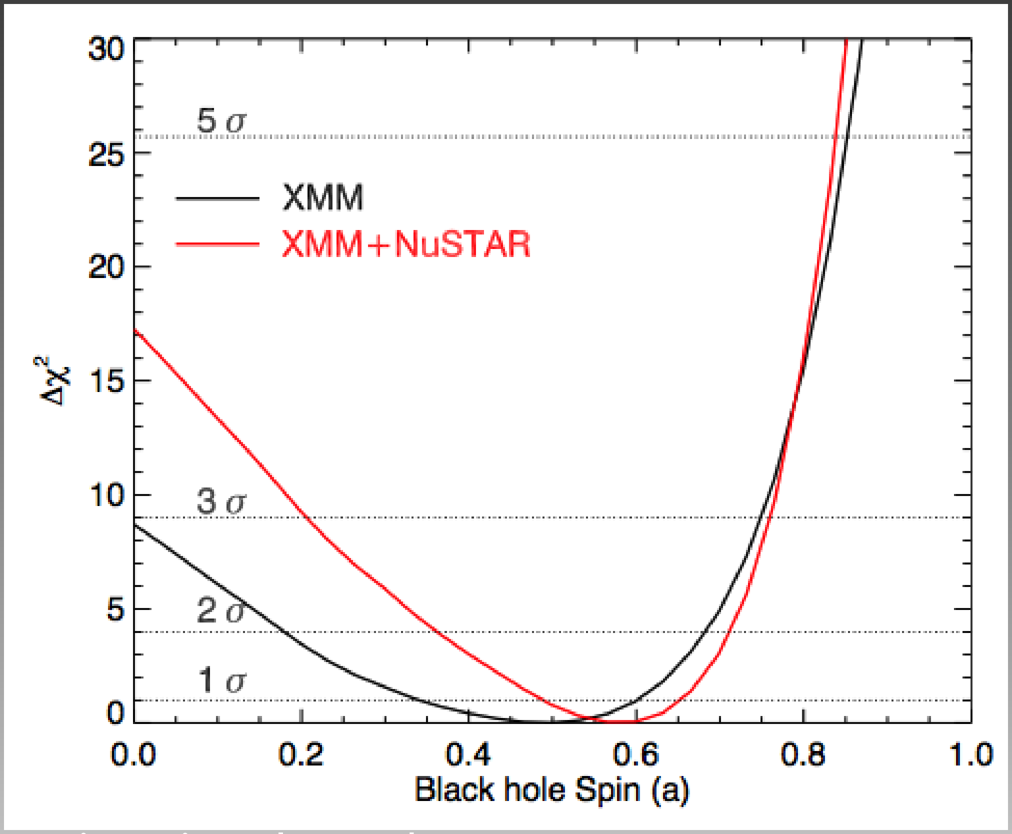

Marinucci et al. 2014b

Thanks to the broad (0.5-80 keV) spectral coverage, we confirmed the intermediate spin value in this source, discarding non-spinning solutions with a significance >3σ

$a=0.58^{+0.11}_{-0.17}$

Outline

- Brief introduction about scientific goals
- Radio-quiet AGN seen by NuSTAR
- Results
- Conclusions

Conclusions

- The recent NuSTAR observational campaign of Radio-quiet AGN allowed us to study:

PRIMARY EMISSION → First measurements of the coronal parameters T and τ in IC 4329A and SWIFT J 2127.4

→ Warm Comptonization in Ark 120 (in addition to reflection?)

REPROCESSED EMISSION → Robust detection and clear discrimination between relativistic and cold reflection

→ Black hole spin measurements in a number of sources: MCG—6-30-15, NGC 1365, Mrk335 and SWIFT J2127.4

- Bringing the two pieces of information together we have an unprecedented powerful tool to investigate the innermost environment (corona and accretion disk) of the nucleus